

Published in final edited form as:

Chem Commun (Camb). 2010 March 21; 46(11): 1851–1853. doi:10.1039/b923711a.

A small library of DNA-encapsulated supramolecular nanoparticles for targeted gene delivery†

Hao Wang^{*}, Kuan-Ju Chen, Shutao Wang, Minori Ohashi, Ken-ichiro Kamei, Jing Sun, Ji Hoon Ha, Kan Liu, and Hsian-Rong Tseng^{*}

Department of Molecular and Medical Pharmacology, Crump Institute for Molecular Imaging (CIMI), Institute for Molecular Medicine (IMED), California NanoSystems Institute (CNSI), University of California, Los Angeles, 570 Westwood Plazas, CNSI Building, Los Angeles, CA 90095-1770, USA.

Abstract

We demonstrated a convenient, flexible and modular synthetic approach for preparation of a small library of DNA encapsulated supramolecular nanoparticles SNPs⊃DNA and RGD-SNPs⊃DNA with different sizes and RGD target ligand coverage for targeted gene delivery.

Gene therapy generally requires delivery vehicles that are capable of (i) carrying/protecting genetic materials, e.g., DNA and siRNA, and (ii) target-specific delivery to desired tissues or subsets of cells.¹ Over the past decades, significant endeavors have been devoted to develop non-viral gene delivery vehicles^{2,3} as alternatives to their viral counterparts, whose applications are restricted due to the potential safety issues and complex processes of preparing. Among the existing non-viral gene delivery systems,^{4–8} nanoparticle-based gene delivery vehicles^{9–12} have received extensive attention.

Recently, we developed a novel assembly approach¹³ for the preparation of size-controllable supramolecular nanoparticles (SNPs) via multivalent molecular recognition based on β-cyclodextrin (CD) and adamantane (Ad) motifs. A collection of SNPs with sizes ranging from 30 to 450 nm were prepared by mixing three molecular building blocks, including (i) cationic Ad-grafted polyamidoamine dendrimer (**Ad-PAMAM**), (ii) cationic CD-grafted branched polyethylenimine (**CD-PEI**) and (iii) Ad-grafted polyethylene glycol (**Ad-PEG**), all at different concentrations. Given the fact that the interior of **SNPs** is composed of a cationic **Ad-PAMAM/CD-PEI** hydrogel network, it is conceivable that **SNPs** can encapsulate anionic plasmid DNA *via* electrostatic interactions. This new type of gene delivery system can provide significant protection of the encapsulated DNA from degradation in an extracellular context.

Here, we adopted this supramolecular assembly approach to prepare a small library of DNA-encapsulated **SNPs** (**SNPs⊃DNA** and **RGD-SNPs⊃DNA**, Scheme 1) with controllable sizes and tunable surface coverage of a targeting ligand, i.e., arginine-glycine-aspartic (**RGD**) peptide. A two-step preparation process has been developed to first generate both 100 and 300 nm **SNPs⊃DNA** from **Ad-PAMAM**, **CD-PEI**, **Ad-PEG** and **DNA**, followed by in situ **RGD** ligand exchange of **SNPs⊃DNA** to give six different **RGD-SNPs⊃DNA** with ligand coverage of 1, 5 and 10 mol% (based on **Ad-PEG**). In this proof-of-concept study, a plasmid

†Electronic supplementary information (ESI) available: Preparation and characterization of **SNPs⊃DNA** and **RGD-SNPs⊃DNA**, electrophoresis analysis, ethidium bromide exclusion assay, dynamic light scattering experiments, and gene transfection protocol. See DOI: 10.1039/b923711a

DNA encoded with an enhanced green fluorescent protein (**EGFP**) driven by a **CMV** promoter was used as a reporter system, and the **RGD** ligand¹⁴ was employed to recognize the $\alpha_v\beta_3$ integrin receptor on the membranes of certain types of tumor cells. To characterize the sizes, morphologies and surface charges of the resulting **SNPs**ⓉDNA and **RGD-SNPs**ⓉDNA, we carried out dynamic light scattering (**DLS**), transmission electron microscope (**TEM**) and zeta potential measurements, respectively. Finally, the gene transfection efficiency and specificity of each **SNPs**ⓉDNA and **RGD-SNPs**ⓉDNA in the small library were examined using $\alpha_v\beta_3$ high-expressed and low-expressed cells, along with the control delivery systems.

We first determined the DNA loading capacity to be used for preparation of **SNPs**ⓉDNA and **RGD-SNPs**ⓉDNA. Similar to cationic polymer based gene delivery systems,^{15,16} the DNA loading capacity of **SNPs** depends on the net cationic charges embedded in the interior Ad-PAMAM/CD-PEI hydrogel network. We utilized both electrophoresis analysis¹⁷ and ethidium bromide exclusion assay¹⁸ to measure the DNA loading capacity of the **Ad-PAMAM/CD-PEI** hydrogel (Fig. S1 and S2; ESI†), resulting in the respective nitrogen/ phosphate (N/P) ratios of 2.6 and 5.0. The N/P ratio of 5.0 was chosen to ensure complete DNA encapsulation in our studies. Next, **SNPs**ⓉDNA with 100 and 300 nm diameters were prepared separately by slowly adding a PBS solution (pH = 7.2) of **CD-PEI** (600 nM) into **PBS** solution containing **Ad-PAMAM** (300 nM for 100 nm **SNPs**ⓉDNA and 600 nM for 300 nm **SNPs**ⓉDNA), **Ad-PEG** (3 μ M) and DNA (2.2 nM), followed by incubation at room temperature for 20 min. The **DLS** measurements indicated that the hydro-dynamic sizes of the 100 and 300 nm **SNPs**ⓉDNA were 106 ± 14 and 312 ± 47 nm, respectively. Subsequently, the samples of each size of **SNPs**ⓉDNA were split into four aliquots, and three of them were subjected to the *in situ* ligand exchange by adding 30, 150 or 300 nM of **RGD-PEG-Ad** (Scheme S1; ESI†). A collection of **RGD-SNPs**ⓉDNA with different **RGD** coverage,¹⁹ namely 100-1%, 100-5%, 100-10%, 300-1%, 300-5% and 300-10%, were obtained accordingly. After *in situ* ligand exchange, the hydrodynamic sizes of **RGD-SNPs**ⓉDNA exhibited negligible changes ($\leq 5\%$, Fig. S4; ESI†). The morphologies of **SNPs**ⓉDNA and **RGD-SNPs**ⓉDNA were then examined by using **TEM**. The **TEM** images (Fig. 1) showed smaller sizes (62.8 for 100 nm **SNPs**ⓉDNA and 210 ± 24 nm for 300 nm **SNPs**ⓉDNA), spherical shapes and narrow size distributions of **SNPs**ⓉDNA and **RGD-SNPs**ⓉDNA. Zeta potential measurements indicated that the surface-charge densities of 100 and 300 nm **SNPs**ⓉDNA were 3.7 ± 0.4 and 6.8 ± 0.5 mV, respectively. After ligand exchange, small increases (3–11%) in zeta potentials of **RGD-SNPs**ⓉDNA were observed (Fig. S5; ESI†).

We carried out an *in vitro* **EGFP** transfection study of a collection of **SNPs**ⓉDNA and **RGD-SNPs**ⓉDNA along with the controls, i.e., DNA, DNA complexes of **CD-PEI**, **CD-PEI/ Ad-PEG** and **RGD-jet-PEI**, in 8-well chamber slides containing two $\alpha_v\beta_3$ high-expressed cells (i.e., U87 and scraping-collected 3T3 cells)²⁰ and two $\alpha_v\beta_3$ low-expressed cells (i.e., **MCF7** and 0.25% trypsin-treated 3T3 cells).²¹

For the purpose of comparison, an equal amount of **EGFP**-encoded plasmid DNA (100 ng) was added to individual cell culture chambers in this transfection study. The resulting 48 individual **EGFP** transfection experiments were incubated at 37 °C (5% CO₂) for 24 h. After para-formaldehyde fixation and DAPI nuclear staining, a fluorescence microscope was used to quantify the **EGFP** expression levels in individual cells. These levels were then used to determine the transfection efficiency for each vehicle. The transfection study was repeated three times, and the results of average transfection efficiency of gene delivery vehicles for different cell lines were summarized in Fig. 2. First, DNA complexes based on each of the molecular

†Electronic supplementary information (ESI) available: Preparation and characterization of **SNPs**ⓉDNA and **RGD-SNPs**ⓉDNA, electrophoresis analysis, ethidium bromide exclusion assay, dynamic light scattering experiments, and gene transfection protocol. See DOI: 10.1039/b923711a

building blocks (**CD-PEI** and **CD-PEI/Ad-PEG**) gave very poor transfection performance similar to free plasmid DNA, indicating that the formation of supramolecular nanoparticles is crucial for achieving enhanced transfection efficiency. Second, it is apparent that 100-nm **RGD-SNPs**ⓁDNA exhibited higher transfection efficiency than those of 300-nm analogues. This observation is consistent with the results from the reported polymer-based gene delivery systems,^{22–24} in which vehicles with 10–100 nm size range display better gene transfection efficiency.¹³ Third, 100-5% **RGD-SNPs**ⓁDNA gave the highest transfection efficiency compared to those observed for **SNPs**ⓁDNA and other targeted **RGD-SNPs**ⓁDNA. The reduced transfection efficiency observed for **100-10% RGD-SNPs**ⓁDNA can be attributed to an excess amount of free **RGD** ligand in the culture medium, which compromised the targeted binding of **RGD-SNPs**ⓁDNA as a result of a competition effect.¹¹ Overall, **100-5% RGD-SNPs**ⓁDNA demonstrated the best transfection efficiencies ($57 \pm 11\%$ and $31 \pm 8\%$ for $\alpha_v\beta_3$ high-expressed 3T3 and U87, respectively). These results are comparable to those observed for the commercially available **RGD-jet-PEI** ($64 \pm 15\%$ and $38 \pm 9\%$ for $\alpha_v\beta_3$ high expressed 3T3 and U87, respectively), which is a well-known selective and efficient transfection reagent for integrin-expressing cell lines.²⁵ Fourth, in addition to high transfection efficiency, **100-5% RGD-SNPs**ⓁDNA also exhibited outstanding delivery specificity to the $\alpha_v\beta_3$ high expressed cells, U87 ($31 \pm 8\%$) and 3T3 ($57 \pm 11\%$), over the $\alpha_3\beta_3$ low expressed cells, **MCF7** ($21 \pm 6\%$) and trypsin-treated 3T3 ($15 \pm 4\%$). Four-fold difference in transfection efficiencies were observed for **100-5% RGD-SNPs**ⓁDNA between $\alpha_v\beta_3$ high-expressed and $\alpha_v\beta_3$ low expressed 3T3 cells, while only 1.2-fold difference was observed for **RGD-jet-PEI**. In contrast to non-target-specific transfection performance of **RGD-jet-PEI**, **100-5% RGD-SNPs**ⓁDNA had higher transfection efficiency for the U87 cell line with respect to the **MCF7** cell line, which indicated good transfection specificity of **RGD-SNPs**ⓁDNA for the $\alpha_v\beta_3$ high expressed cell lines. Moreover, we tested the toxicity of **SNPs**ⓁDNA and **RGD-SNPs**ⓁDNA by using the cell viability assay. The cells transfected by **SNPs**ⓁDNA and **RGD-SNPs**ⓁDNA were compared with the cells cultured in the normal medium. There were no significant differences in viability ($97 \pm 2\%$), which suggested that the toxicity of **SNPs**ⓁDNA and **RGD-SNPs**ⓁDNA is negligible for *in vitro* transfection studies (Fig. S6, ESI†).

In conclusion, we demonstrated a convenient, flexible and modular synthetic approach for preparation of a small library of **SNPs**ⓁDNA and **RGD-SNPs**ⓁDNA with different sizes and **RGD** ligand coverage. Gene transfection studies of **SNPs**ⓁDNA and **RGD-SNPs**ⓁDNA library for $\alpha_v\beta_3$ high-expressed cells and $\alpha_v\beta_3$ low-expressed cells were performed. The results revealed that the size and target ligand coverage of **RGD-SNPs**ⓁDNA played a critical role in the target-specific gene delivery. In conjunction with the use of a miniaturized high throughput screening platform²⁶ and molecular imaging technology,¹³ we will dramatically accelerate the discovery processes of **SNPs**-based gene delivery vehicles toward *in vivo* application.

Supplementary Material

Refer to Web version on PubMed Central for supplementary material.

Acknowledgments

This research was supported by NIH-NCI NanoSystems Biology Cancer Center (U54CA119347) and NIH R21 grant (EB008419-01). We appreciate the reviewers suggestive comments to help us improve our manuscript.

Notes and references

1. Kim DH, Rossi JJ. Nat. Rev. Genet 2007;8:173–84. [PubMed: 17304245]

2. Glover DJ, Lipps HJ, Jans DA. *Nat. Rev. Genet* 2005;6:299–310. [PubMed: 15761468]
3. Rosi NL, Mirkin CA. *Chem. Rev* 2005;105:1547–1562. [PubMed: 15826019]
4. Niidome T, Huang L. *Gene Ther* 2002;9:1647–1652. [PubMed: 12457277]
5. Prata CAH, Li Y, Luo D, McIntosh TJ, Barthelemy P, Grinstaff MW. *Chem. Commun* 2008:1566–1568.
6. Woodrow KA, Cu Y, Booth CJ, Saucier-Sawyer JK, Wood MJ, Saltzman WM. *Nat. Mater* 2009;8:526–533. [PubMed: 19404239]
7. Chen Y, Yu L, Feng Z, Hou S, Liu Y. *Chem. Commun* 2009:4106–4108.
8. Torchilin VP, Levchenko TS, Rammohan R, Volodina N, Papahadjopoulos-Sternberg B, D'Souza GG. *Proc. Natl. Acad. Sci. U. S. A* 2003;100:1972–1977. [PubMed: 12571356]
9. Liang H, Harries D, Wong GC. *Proc. Natl. Acad. Sci. U.S.A* 2005;102:11173–11178. [PubMed: 16061807]
10. Kumar A, Kumar V. *Chem. Commun* 2009:5433–5435.
11. Bazin L, Gressier M, Taberna PL, Menu MJ, Simon P. *Chem. Commun* 2008:5004–5006.
12. Cheon J, Lee JH. *Acc. Chem. Res* 2008;41:1630–1640. [PubMed: 18698851]
13. Wang H, Wang ST, Su H, Chen KJ, Armijo AL, Lin WY, Wang YJ, Sun J, Kamei K, Czernin J, Radu CG, Tseng HR. *Angew. Chem., Int. Ed* 2009;48:4344–4348.
14. Liu Z, Cai WB, He LN, Nakayama N, Chen K, Sun XM, Chen XY, Dai HJ. *Nat. Nanotechnol* 2007;2:47–52. [PubMed: 18654207]
15. Srinivasachari S, Reineke TM. *Biomaterials* 2009;30:928–938. [PubMed: 19027153]
16. Li J, Yang C, Li HZ, Wang X, Goh SH, Ding JL, Wang DY, Leong KW. *Adv. Mater* 2006;18:2969–2970.
17. Zugates GT, Anderson DG, Little SR, Lawhorn IEB, Langer R. *J. Am. Chem. Soc* 2006;128:12726–12734. [PubMed: 17002366]
18. Meyer M, Philipp A, Oskuee R, Schmidt C, Wagner E. *J. Am. Chem. Soc* 2008;130:3273–3273.
19. When mixing ratios of RGD to target ligand were 1, 5 and 10%, the actual RGD ligand coverages on the 100 nm **RGD-SNPs**⊃**DDNA** were $0.8 \pm 0.2\%$, $2.9 \pm 0.5\%$ and $6.7 \pm 0.8\%$, respectively. For 300 nm **RGD-SNPs**⊃**DDNA**, the RGD ligand coverages were $0.9 \pm 0.2\%$, $2.2 \pm 0.4\%$ and $6.7 \pm 0.6\%$, respectively. For details see ESI†.
20. Ng QKT, Sutton MK, Soonsawad P, Xing L, Cheng H, Segura T. *Mol. Ther* 2009;17:828–836. [PubMed: 19240693]
21. Xie J, Chen K, Lee HY, Xu CJ, Hsu AR, Peng S, Chen XY, Sun SH. *J. Am. Chem. Soc* 2008;130:7542–7543. [PubMed: 18500805]
22. Davis ME, Chen Z, Shin DM. *Nat. Rev. Drug Discovery* 2008;7:771–782.
23. Yu HJ, Wagner E. *Curr. Opin. Mol. Ther* 2009;11:165–178. [PubMed: 19330722]
24. Fukushima S, Miyata K, Nishiyama N, Kanayama N, Yamasaki Y, Kataoka K. *J. Am. Chem. Soc* 2005;127:2810–2811. [PubMed: 15740090]
25. Erbacher P, Remy JS, Behr JP. *Gene Ther* 1999;6:138–45. [PubMed: 10341886]
- 26 (a). Lin W-Y, Wang Y, Wang S, Tseng H-R. *Nano Today* 2009;4:470–481. [PubMed: 20209065] (b) Wang YJ, Lin WY, Liu K, Lin RJ, Selke M, Kolb HC, Zhang NG, Zhao XZ, Phelps ME, Shen CKF, Faull KF, Tseng HR. *Lab Chip* 2009;9:2281–2285. [PubMed: 19636457] (c) Wang J, Sui G, Mocharla VP, Lin RJ, Phelps ME, Kolb HC, Tseng H-R. *Angew. Chem., Int. Ed* 2006;45:5276–5281.

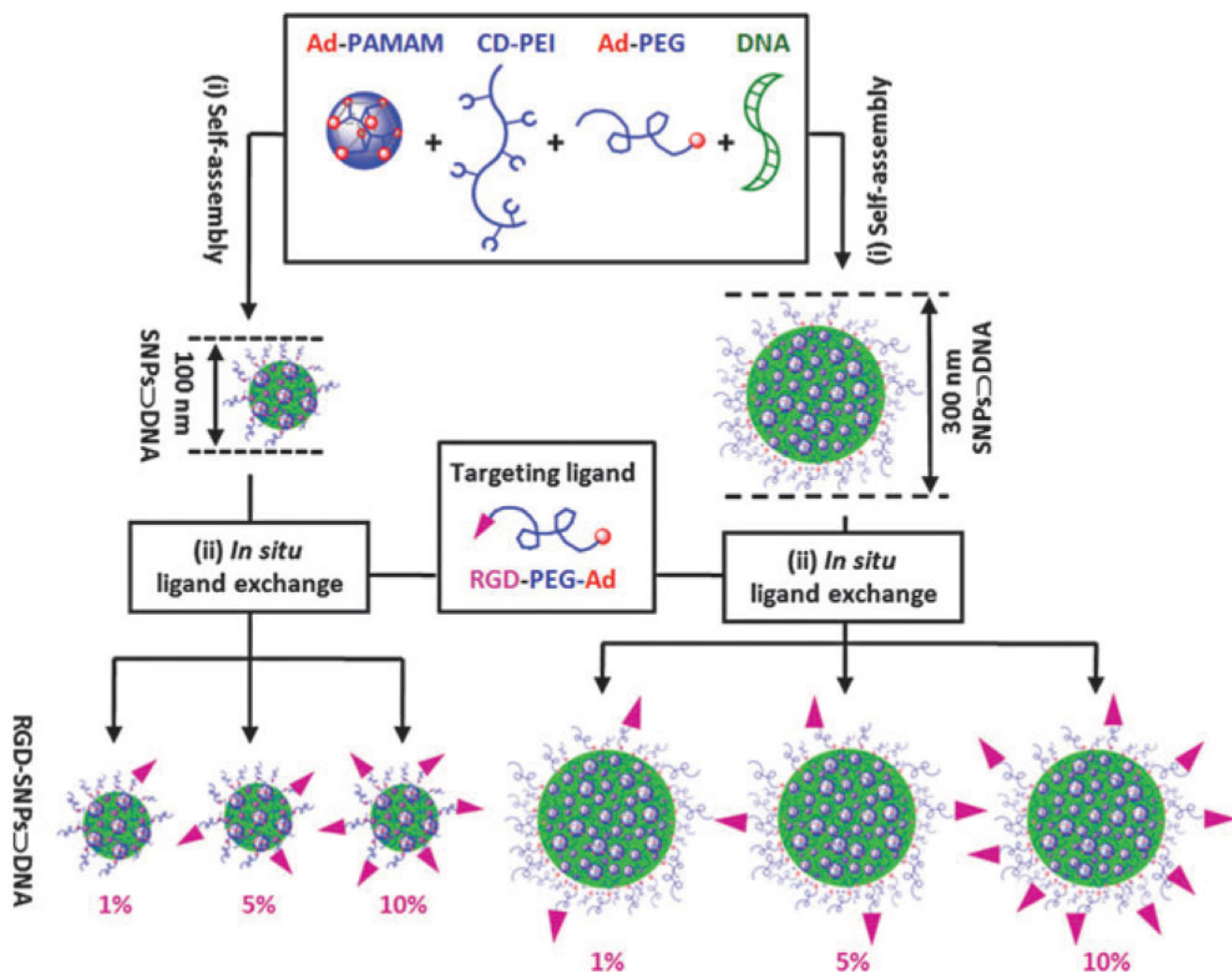


Fig. 1. TEM micrographs of (a) 100 nm SNPs@DNA and (b) 300 nm SNPs@DNA. Insets: the respective higher magnification TEM images. Scale bars: 100 nm. (c) and (d) Histograms summarize the size distributions of 100 nm SNPs@DNA and 300 nm SNPs@DNA in dry states.

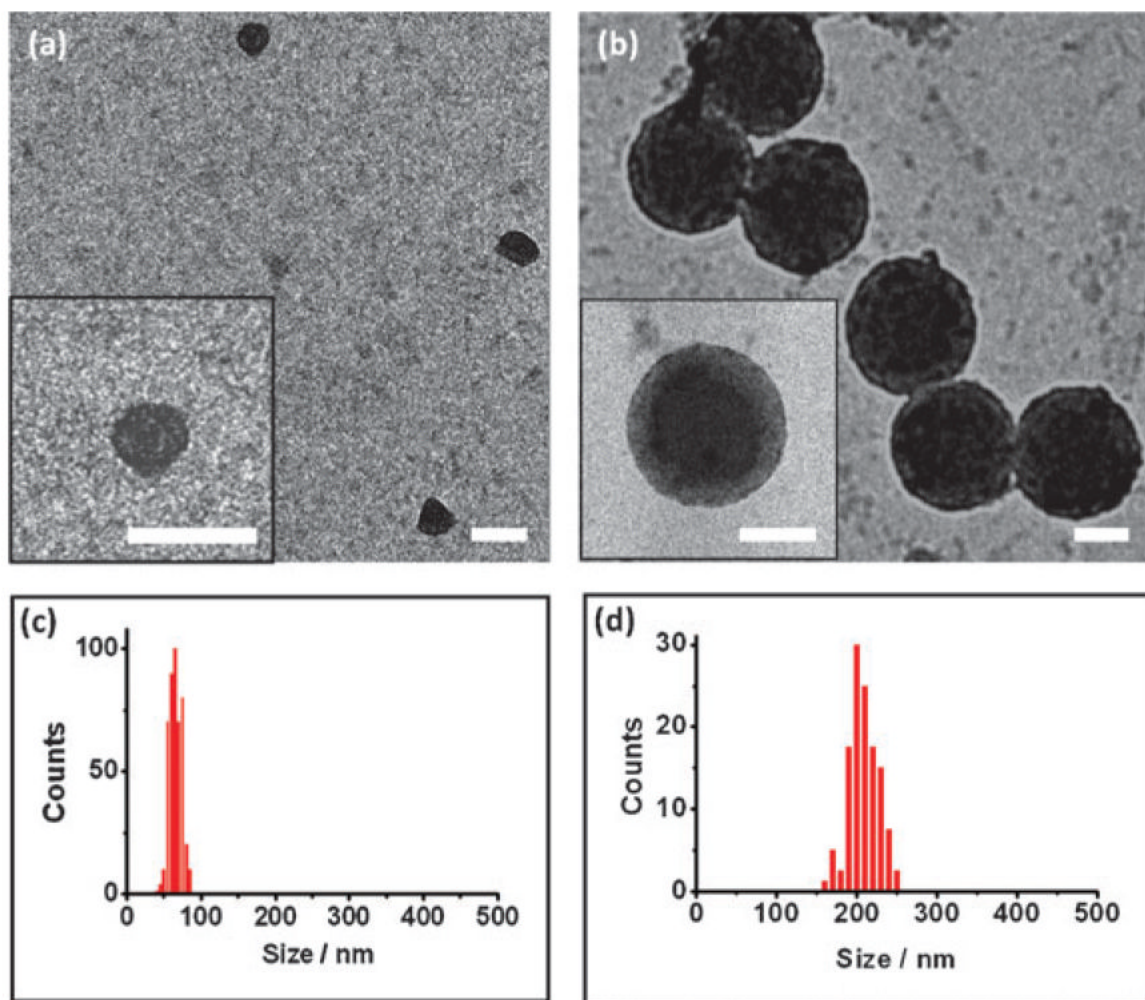
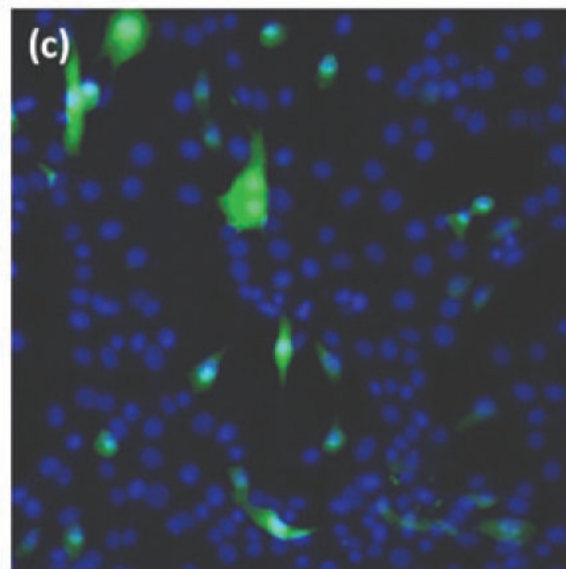
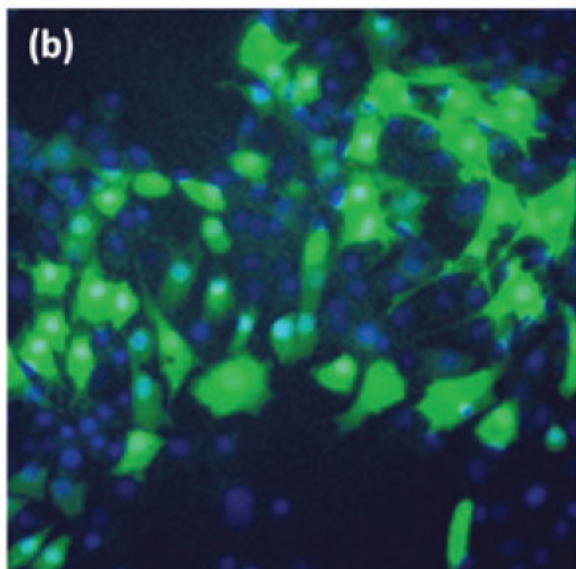
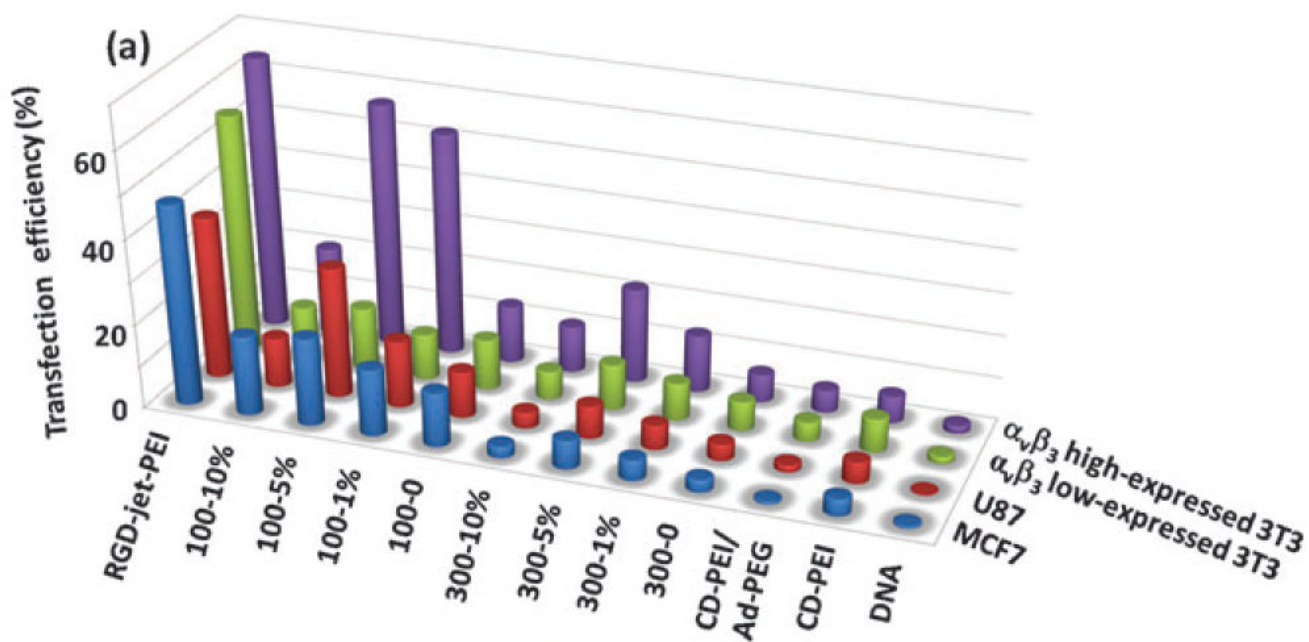


Fig. 2.

(a) EGFP transfection efficiency of a collection of **SNPs** and **RGD-SNPs** along with control delivery systems for two $\alpha_v\beta_3$ high-expressed cells (U87 and scraping-collected 3T3 cells) and two $\alpha_v\beta_3$ low-expressed cells (**MCF7** and 0.25% trypsin-treated 3T3 cells). The representative fluorescence micrographs of $57 \pm 11\%$ and $9 \pm 4\%$ transfection efficiencies observed for (b) 5 mol% RGD-grafted 100 nm **RGD-SNPs** (**100-5%**)-treated $\alpha_v\beta_3$ high-expressed 3T3 cells and (c) 1 mol% RGD-grafted 300 nm **RGD-SNPs** (**300-1%**)-treated $\alpha_v\beta_3$ low-expressed 3T3 cells.



Scheme 1.

A two-step modular assembly approach for preparation of a small library of DNA-encapsulated supramolecular nanoparticles (SNPs \rightarrow DNA and RGD-SNPs \rightarrow DNA) with controllable sizes and tunable RGD ligand coverage.